Mechanisms Behind the Generation of Protonated Ions for Polyaromatic Hydrocarbons by Atmospheric Pressure Photoionization

ARTICLE *in* ANALYTICAL CHEMISTRY · DECEMBER 2011

Impact Factor: 5.64 · DOI: 10.1021/ac202858k · Source: PubMed

4 AUTHORS:

Arif Ahmed
Kyungpook National University
12 PUBLICATIONS **100** CITATIONS
SEE PROFILE

Cheol Ho Choi
Kyungpook National University
111 PUBLICATIONS **2,123** CITATIONS
SEE PROFILE

Myoung choul Choi
Korea Basic Science Institute KBSI
35 PUBLICATIONS **98** CITATIONS
SEE PROFILE

Sunghwan Kim
Kyungpook National University
66 PUBLICATIONS **2,228** CITATIONS
SEE PROFILE

analytical chemistry

Article

pubs.acs.org/ac

Mechanisms Behind the Generation of Protonated Ions for Polyaromatic Hydrocarbons by Atmospheric Pressure Photoionization

Arif Ahmed,[†] Cheol Ho Choi,[†,‡] Myoung Choul Choi,[§] and Sunghwan Kim*[,†,‡]

[†]Department of Chemistry, Kyungpook National University, Daegu, 702-701, Republic of Korea

[‡]Green-Nano Materials Research Center, Daegu, 702-701, Republic of Korea

[§]Korean Basic Science Institute, Ochang-Eup, 804-1, Republic of Korea

Supporting Information

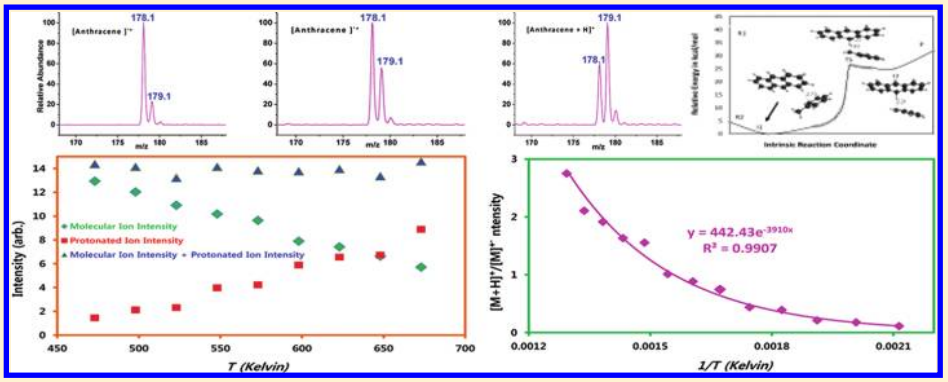

ABSTRACT: In this study, the mechanism behind the generation of protonated polyaromatic hydrocarbon (PAH) ions without heteroatoms by atmospheric pressure photoionization (APPI) is investigated. Comparing data obtained by APPI of anthracene dissolved either in toluene or perdeuterated toluene suggests that toluene acts as a source of protons and that breakage of C−H bonds in the toluene molecule is important for the overall protonation reaction. Our data describing an Arrhenius-type temperature-dependent relationship between the signal intensities of molecular and protonated ions suggest a mechanistic relation between the generated molecular and protonated ions. The APPI protonation mechanism that best explains the observed phenomena is composed of two reactions: electron transfer followed by hydrogen transfer. This two-step mechanism for APPI was originally suggested by Syage (Syage, J. A. *J. Am. Soc. Mass Spectrom.* **2004**, *15*, 1521−1533). Further quantum mechanical study shows that an energetically favorable ion−molecular complex can be generated as a result of electron transfer from toluene to PAH, which subsequently facilitates hydrogen transfer. This suggests that both electron transfer and hydrogen transfer can occur as a "concerted" reaction through the ion−molecular complex precursor state, which is consistent with experimental results. To our best knowledge, this is the first time that the dynamic nature of the APPI process is clearly revealed by combined experimental and quantum mechanical studies.

Recently, mass spectrometry (MS) has become an essential tool widely utilized in numerous applications across many disciplines.[1−6] In MS, the ionization process is one of the main determinants of sensitivity and quality of obtained data as most mass analyzers measure the mass-to-charge ratios of analytes using electrostatic and magnetic fields. Atmospheric pressure photoionization (APPI) is one of the important ionization techniques, and it has been widely used to study humic substances,[7,8] petroleum,[9−11] drugs,[12,13] environmental contaminants,[14,15] nucleic bases, ribonucleosides and ribonucleotides,[16] anthocyanins (wine fingerprints),[17] sulfonamides,[18] mycotoxins,[19] pesticides,[20] antibiotics,[21] steroids,[22] lipids,[23] and halogenated compounds.[24] Considering the importance of the APPI, one can easily understand the previous focus devoted to understanding and improving the APPI technique.[25−35]

During a typical APPI process, molecular and protonated ions are generated in a process that is the subject of some study[26,30,32,36] and debate, and one in which general agreement on the exact ionization mechanism has not yet been reached. In work published by Syage,[30] protonated ions were reported to be generated via electron transfer followed by hydrogen transfer. The author also concluded that hydrogen was likely donated by the solvent. In another study by Kauppila et al.,[26] protonation reportedly occurs by direct protonation from dopant radical ions, with the authors suggesting that the proton came from the solvent. In another study published by Purcell et al.,[32]

Received: October 29, 2011
Accepted: December 15, 2011
Published: December 15, 2011

the APPI mechanism applied to a basic compounds mixture in toluene was investigated, whereby the authors concluded that protons originated not from toluene but from the mixture itself. In a recent study published by Panda et al.,[36] water and oxygen molecules were suggested to play an important role in the APPI process

One of the reasons for this discrepancy between suggested mechanisms may be attributable to the complex nature of the APPI process. In other words, the exact APPI mechanism may be different depending on the choice of solvent and analytes. Therefore, it is beneficial to study the APPI process systematically first by utilizing a selected combination of solvent and analytes, and later employing more variety of solvents and analytes. In this study, the APPI mechanism for the protonation of polyaromatic hydrocarbon (PAH) compounds without heteroatoms dissolved in toluene was chosen to be investigated by use of MS and molecular simulation. In this report, the kinetic isotope effect and an Arrhenius-type temperature-dependent ion generation is invoked to explain the APPI mechanism. Additionally, a newly reported mechanism that better describes the experimental and simulation data is suggested.

EXPERIMENTAL SECTION

MS Analysis. Anthracene, acenaphthalene, phenanthrene, pyrene, fluoranthene, benz(*b*)anthracene, benzo(*b*)fluoranthene, HPLC-grade toluene, and deuterated toluene were purchased from Sigma-Aldrich (St. Louis, MO, U.S.A.) and used without further purification. Deuterated anthracene was obtained from Cambridge Isotope Laboratories (Andover, MA, U.S.A.). Standard samples were dissolved in toluene to a final concentration of ~10 μM. These solutions were analyzed using a positive-mode APPI LCQ Fleet ion trap mass spectrometer (Thermo Scientific, Waltham, MA, U.S.A.). All solutions were directly injected into the APPI source using a Harvard syringe pump model 11 (Harvard, Holliston, MA, U.S.A.) at a flow rate of 40 μL/min; the vaporizer temperature was controlled between 200 and 400 °C. And the other operating mass spectrometric parameters were as follows: sheath, aux, and sweep gas flow rate (arb) = 10, 5, and 0, respectively, capillary temperature 300 °C, capillary voltage 15 V, and tube lens 70 V. High-purity nitrogen gas obtained from a liquid nitrogen Dewar was used for both a sheath and auxiliary gas for the ionization source.

Computational Details. Density functional theory with B3LYP functionals was utilized in combination with an all-electron 6-31G(d,p)[37] basis set. Minimum energy reaction paths were determined by first optimizing the geometries of the minima and transition states. Each stationary point was characterized by computing and diagonalizing its Hessian matrix (matrix of energy second derivatives). Minima (first-order saddle points) are characterized by Hessians with 0(1) negative eigenvalues. To follow the minimum energy path (MEP), also called the intrinsic reaction coordinate (IRC), the Gonzalez–Schlegel second-order method[38] was used with a step size of 0.3 amu$^{1/2}$ bohr. The general atomic and molecular electronic structure system[39] (GAMESS) program was used for all of the computations.

RESULTS AND DISCUSSION

Investigation of the Proton Source. Anthracene dissolved either in toluene or deuterated toluene was analyzed by (+) mode APPI MS; the resultant spectra are displayed in Figure 1, parts a and b. All other experimental conditions, except choice of solvent, were identical. Protonated ions are dominant in a spectrum obtained from anthracene dissolved in toluene (Figure 1a). However, molecular ions are dominant in

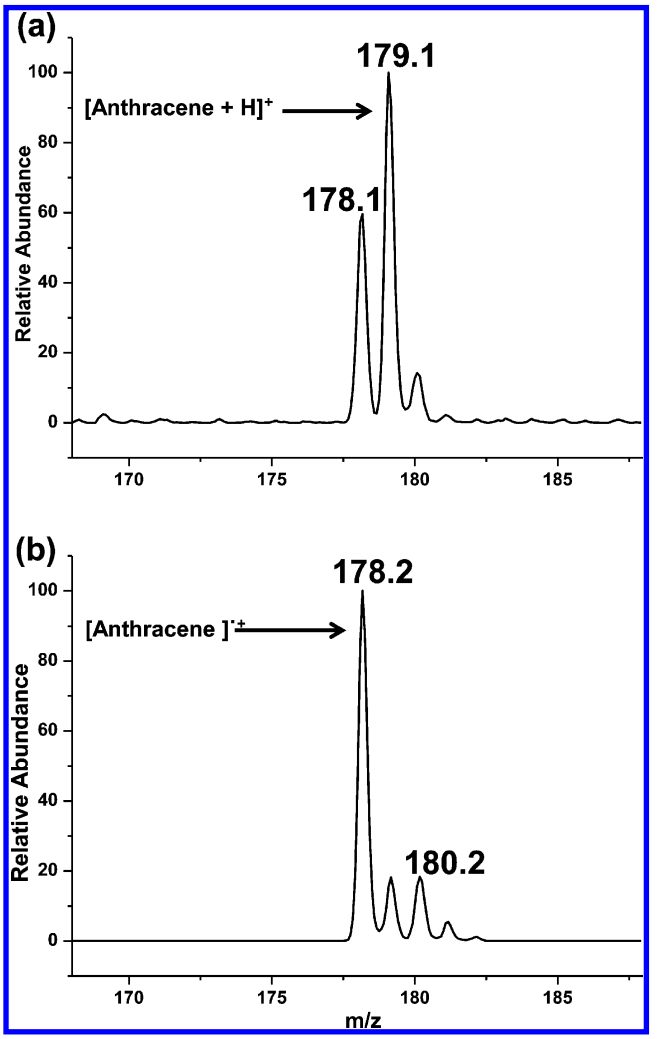

Figure 1. APPI positive ion mass spectra of anthracene dissolved in toluene (a) and anthracene in perdeuterated toluene (b).

a spectrum obtained from a deuterated toluene solvent, with protonated and deuterated ions much less abundant (Figure 1b). Two facts can be deduced by comparing the two spectra present in Figure 1. The first is that toluene is the source of protons used in the generation of protonated anthracene ions. If this was not the case, and the proton came from a different source, such as residual water in the ionization source and not from toluene, the anthracene should have produced protonated ions even when the solvent was switched to deuterated toluene. However, protonated ions were generated only with normal toluene, and not with deuterated solvent, and other possible proton sources such as residual water can be eliminated. Second, the data suggest that the protonation reaction can be kinetically controlled. Figure 1 clearly shows that substitution of hydrogen to deuterium atoms in toluene greatly influences the protonation reaction. This finding, combined with considering the well-known kinetic isotope effect, suggests that breakage of C–H is important to determine overall reaction rate. According to the kinetic isotope effect, the activation energy for the breakage of the C–D bond is higher than that for the C–H bond.[40]

dx.doi.org/10.1021/ac202858k | *Anal. Chem.* 2012, 84, 1146–1151

Temperature Dependence of Generating Protonated PAH. To further clarify the protonation mechanism, the temperature dependence of the protonation reaction was monitored by varying the vaporizer temperature of the APPI source. The vaporizer temperature is used to heat up the solvent and analyte, evaporating them into the gas phase. Anthracene dissolved in toluene was analyzed under various vaporizer temperatures; the resultant spectrum is shown in Figure 2. Molecular ions are clearly dominant at lower

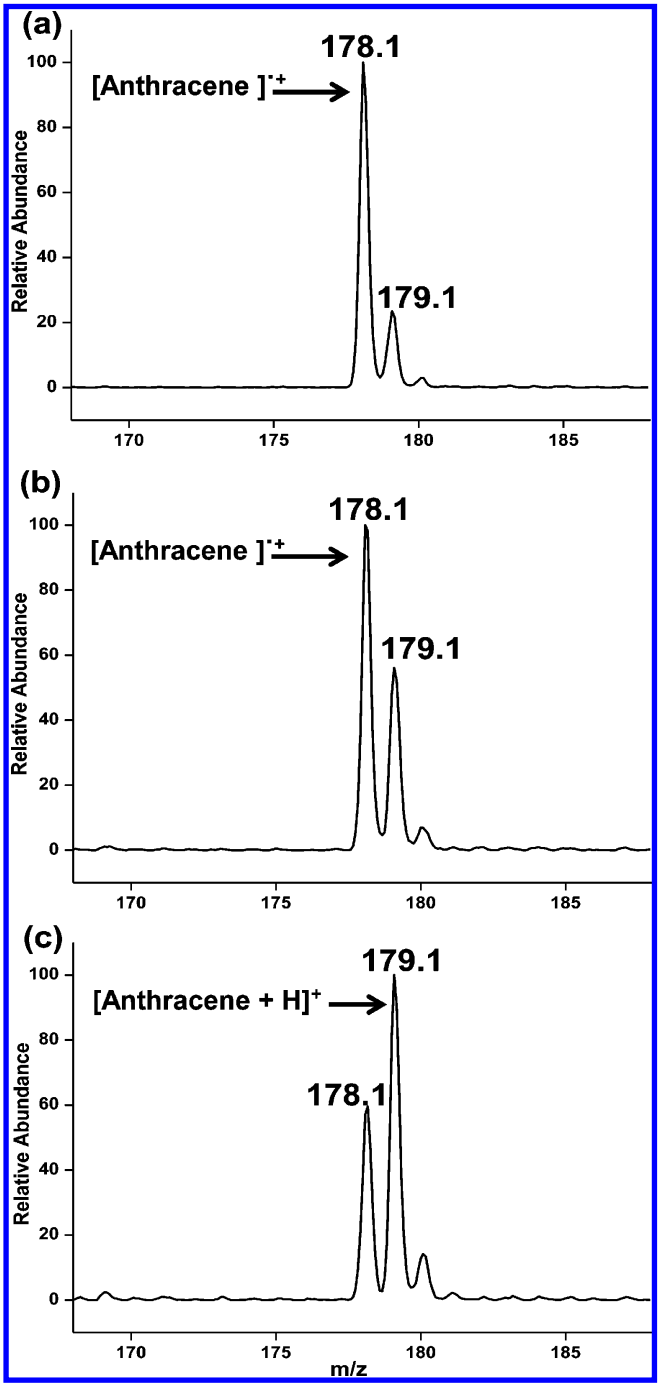

Figure 2. Plots for the temperature-dependent progressive change of peak heights of molecular ($[M]^{+\bullet}$) and protonated ions ($[M + H]^+$) observed in the anthracene APPI spectra.

temperatures (especially at 200−300 °C), whereby protonated ions gradually become dominant as the temperature increases to 400 °C. Abundances of protonated and molecular ions obtained at various temperatures are plotted and shown in Figure 3a; this demonstrates that increasing the temperature

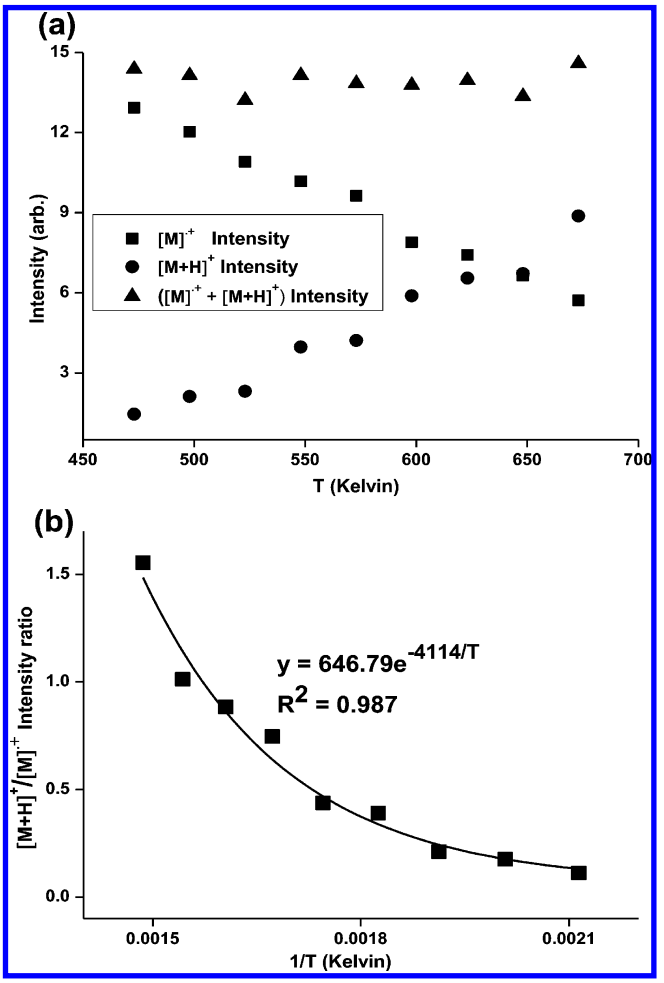

Figure 3. Plots for the temperature-dependent progressive change of (a) the intensity values for $[M]^{+\bullet}$, $[M + H]^+$, and their total sum and (b) $[M + H]^+/[M]^{+\bullet}$ intensity ratios observed in the anthracene APPI spectra.

results in a gradual increase in the abundance of protonated ions with a subsequent decrease in the abundance of molecular ions. The total peak intensity of protonated and molecular ions observed at each temperature is marked in Figure 3a. The summed abundance of each ion remained fairly constant despite temperature variation.

The ratio between the abundance of molecular and protonated ions was obtained and plotted against inverse temperature, as shown in Figure 3b. The abundance of protonated peaks was calculated by subtracting the abundance of molecular ions with a ^{13}C from the abundance of protonated peak observed in Figure 2. The abundance of ^{13}C of molecular ions was calculated by use of the natural abundance of ^{13}C. This figure clearly shows that a function relating this ratio to APPI vaporizer temperature can be described by an expression very similar to the Arrhenius equation. A temperature-dependent experiment was also performed with various analyte concentrations, and it was observed that concentration had no significant effect on the ratio between molecular and protonated ions (refer to Figure S1 in the Supporting Information). The fact that the

dx.doi.org/10.1021/ac202858k | Anal. Chem. 2012, 84, 1146−1151

ratio between molecular (or radical) and protonated ions can be described by a mathematical function clearly shows that the generation of molecular and protonated ions is not independent but is related to each other. Therefore, this finding suggests that the ionization mechanism that produces protonated anthracene includes both molecular and protonated ions.

To determine whether this temperature-dependent behavior is observed with other PAH compounds, experiments were repeated with acenaphthalene, phenanthrene, benz(*b*)-anthracene, pyrene, and fluoranthene. Plots describing these experiments are presented in Figure 4. Note that, although

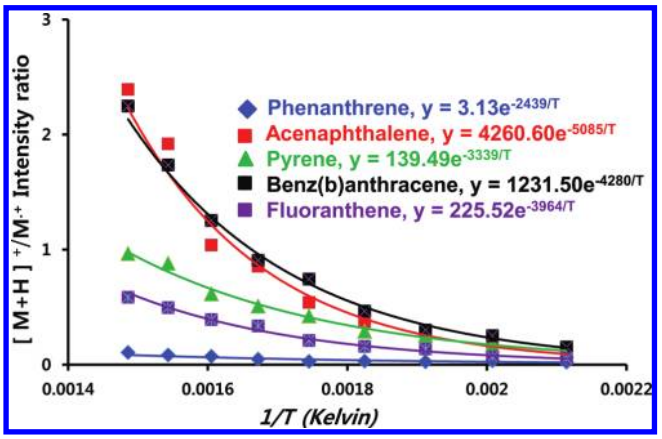

Figure 4. Plot of the temperature-dependent progressive change of $[M + H]^+/[M]^{+\bullet}$ intensity ratio and negative exponential function to fit the APPI spectrum of acenaphthalene, phenanthrene, benz(*b*)-anthracene, pyrene, and fluoranthene.

function coefficients describing curves are different from compound to compound, a similar Arrhenius-type relationship was observed, which suggests that the mechanistic relationship between molecular and protonated ions also exists in the protonation of other PAH compounds. An explanation for relationship between structural or molecular parameter of the molecules and coefficients of the Arrhenius-type curves is not available, and further studies including more standard compounds will be needed to find it.

Mechanistic Considerations. Previously suggested mechanisms[26,30,32,36] are summarized in Figure 5. In a typical APPI

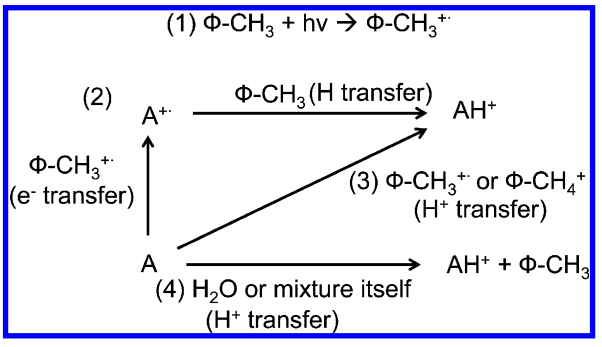

Figure 5. Diagram summarizing suggested reaction pathways from previous studies.

experiment, the molar ratio between analyte (A) and toluene (Φ-CH_3) is >1:100 000. Therefore, the 10 eV photons generated by the Kr lamp are expected to be mostly absorbed by toluene molecules. The absorption of photons will generate toluene radical ions, and the reaction between toluene radical ion and anthracene can produce anthracene radical ions by a charge-exchange reaction[26] (reaction 1 in Figure 5). The protonation of the analyte can be preceded by direct protonation reaction with toluene radical or protonated toluene ions (reactions 3), H_2O[36] or the mixture[32] itself (reaction 4), and by a combination of electron and hydrogen transfer[30] (reaction 2). The difference between paths 3 and 4 is the proton source.

According to data presented in Figure 1, toluene is the proton source for the photoionization of PAHs without heteroatoms. Therefore, reaction 4 is discarded as a major ionization mechanism. Additionally, the data presented in Figures 2 and 3 demonstrate that molecular and protonated ions are not independent of each other but are mechanically related. The thermochemical data for toluene, benzyl radical, and anthracene were obtained from the NIST Webbook[41] and are listed in Table 1. It is shown in the table that the proton affinity (PA) of

Table 1. List of the Thermochemical Data for Toluene, Benzyl Radical, and Anthracene from the NIST Webbook

compound	ionization energy (IE) eV	proton affinity (PA) kJ/mol
toluene	8.8	784.0
benzyl radical	7.2	831.4
anthracene	7.4	877.3

the benzyl radical is larger than the PA of toluene, and hence it is unlikely that the toluene molecular ion can protonate toluene. Therefore, it is less likely that benzyl radical (refer to reaction 3 in Figure 5) is involved in the protonation of anthracene. In conclusion, the only mechanism that can explain Figures 1−3 is the combination of electron and hydrogen transfer originally suggested by Syage.[30]

Computational Studies. To further study the ionization mechanism, analysis by theoretical calculations was performed. The potential energy surface between anthracene and toluene was calculated and is presented in Figure 6. The minima and

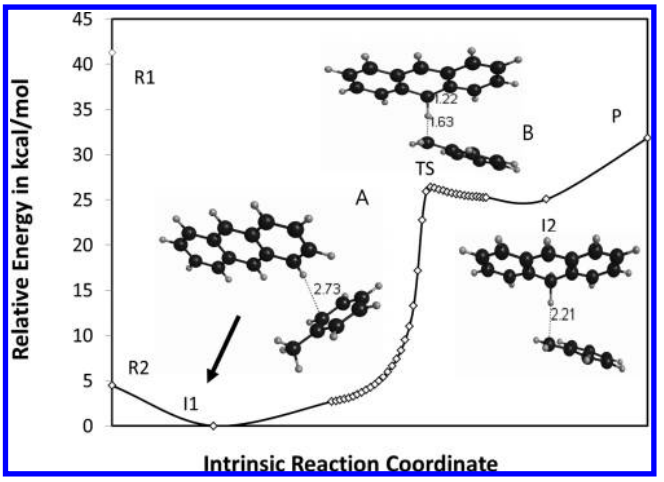

Figure 6. Figure of the potential energy surface between anthracene and toluene obtained by quantum mechanical calculation.

transition states as well as intrinsic reaction coordinates were calculated to study the mechanism in detail. The R1 presents a simple summed molecular energy of separated anthracene and positively charged toluene radical, whereas R2 is the energy of

dx.doi.org/10.1021/ac202858k | *Anal. Chem.* 2012, 84, 1146−1151

separated positively charged anthracene radial and toluene. Therefore, R1 and R2 present ionized toluene and ionized anthracene, respectively. The first intermediate (I1) is a bound structure of anthracene and toluene, which is a positively charged radical. The hydrogen-transfer transition state (TS) was also located on the condition of the positively charged radical. A gas-phase chemical reaction was assumed throughout the calculations.

The quantum mechanical result suggests that the reaction between anthracene and toluene (R1) would immediately produce an anthracene molecular ion and neutral toluene (R2) via electron transfer, since R2 is more stable than R1 by 36.8 kcal/mol. The resulting anthracene molecular ion and toluene (R2) can form an intermediate complex (I1) right after a charge-exchange reaction. The intermediate complex (I1) is more stable than the separated charge-exchange reaction products (R2) by 4.4 kcal/mol. The formation of this intermediate complex (I1) significantly increases the chance of subsequent hydrogen-transfer reaction by improving collision frequencies of reactions. The transition state (TS) that connects the I1 and another intermediate (I2) shows the hydrogen transfer of methyl hydrogen to anthracene with the reaction barrier of 26.4 kcal/mol. With additional thermal energies of 6.8 kcal/mol, the I2 can be converted to the final protonated ions (P). Quantum mechanical calculations of the mechanism show that the ion−molecular complex can be generated immediately following the electron-transfer reaction in an energetically favorable step, which suggests that electron and hydrogen transfer can occur as an apparent "concerted" reaction through the complex.

Despite the endothermic nature of the hydrogen-transfer reaction, the overall protonation reaction is exothermic as the electron-transfer step is very exothermic. From the potential energy surface of the mechanism shown in Figure 6, the generation of molecular ions is expected to be more favored at a lower reaction temperature because the molecular ions cannot overcome the energy barrier to become protonated ions. However, as the reaction temperature increases, the energy barrier for hydrogen transfer can be overcome, resulting in an increase in protonation. This trend agrees well with an Arrhenius-type temperature dependence presented in Figure 3.

CONCLUSIONS

In summary, a mechanism for the photoionization of PAH compounds without heteroatoms dissolved in toluene is defined and presented within. This mechanism is composed of two reactions: electron transfer followed by hydrogen transfer. Subsequent molecular simulation agrees well with experimental data and this suggested mechanism. This simulation shows that an ion−molecule complex can be generated in between two reactions such that the two separate reactions can occur in a concerted manner. The current report shows the potential of combining mass spectrometry and quantum mechanical calculation to study an ionization mechanism. This study provides a fundamental basis toward understanding the APPI mechanism and will be extended to include more compounds (e.g., PAHs with heteroatoms) and solvents to further clarify this complex photoionization process.

ASSOCIATED CONTENT

Supporting Information

Additional information as noted in text. This material is available free of charge via the Internet at http://pubs.acs.org.

AUTHOR INFORMATION

Corresponding Author

*Phone: 82-53-950-5333. Fax: 82-53-950-6330. E-mail: sunghwank@knu.ac.kr.

ACKNOWLEDGMENTS

This work was supported by the Industrial Strategic Technology Development program (10038662, MALDI-TOF for the diagnosis of BRCA mutation and genitourinary infection pathogen) funded by the Ministry of Knowledge Economy (MKE, Korea) and by project no. PM55021 (grant-in-aid from the Ministry of Land, Transport and Maritime Affairs, Korea).

REFERENCES

(1) Stenson, A. C.; Landing, W. M.; Marshall, A. G.; Cooper, W. T. *Anal. Chem.* **2002**, *74*, 4397−4409.
(2) Marshall, A. G.; Rodgers, R. P. *Acc. Chem. Res.* **2004**, *37*, 53−59.
(3) Purcell, J. M.; Hendrickson, C. L.; Rodgers, R. P.; Marshall, A. G. *Anal. Chem.* **2006**, *78*, 5906−5912.
(4) Panda, S. K.; Andersson, J. T.; Schrader, W. *Anal. Bioanal. Chem.* **2007**, *389*, 1329−1339.
(5) Panda, S. K.; Andersson, J. T.; Schrader, W. *Angew. Chem., Int. Ed.* **2009**, *48*, 1788−1791.
(6) Haapala, M.; Purcell, J. M.; Saarela, V.; Franssila, S.; Rodgers, R. P.; Hendrickson, C. L.; Kotiaho, T.; Marshall, A. G.; Kostiainen, R. *Anal. Chem.* **2009**, *81*, 2799−2803.
(7) D'Andrilli, J.; Dittmar, T.; Koch, B. P.; Purcell, J. M.; Marshall, A. G.; Cooper, W. T. *Rapid Commun. Mass Spectrom.* **2010**, *24*, 643−650.
(8) Bae, E.; Yeo, I. J.; Jeong, B.; Shin, Y.; Shin, K.-H.; Kim, S. *Anal. Chem.* **2011**, *83*, 4193−4199.
(9) Hur, M.; Yeo, I.; Kim, E.; No, M.-h.; Koh, J.; Cho, Y. J.; Lee, J. W.; Kim, S. *Energy Fuels* **2010**, *24*, 5524−5532.
(10) Purcell, J. M.; Merdrignac, I.; Rodgers, R. P.; Marshall, A. G.; Gauthier, T.; Guibard, I. *Energy Fuels* **2010**, *24*, 2257−2265.
(11) Cho, Y.; Kim, Y. H.; Kim, S. *Anal. Chem.* **2011**, *83*, 6068−6073.
(12) Hakala, K. S.; Laitinen, L.; Kaukonen, A. M.; Hirvonen, J.; Kostiainen, R.; Kotiaho, T. *Anal. Chem.* **2003**, *75*, 5969−5977.
(13) Cai, Y.; Kingery, D.; McConnell, O.; Bach, A. C. *Rapid Commun. Mass Spectrom.* **2005**, *19*, 1717−1724.
(14) Itoh, N.; Aoyagi, Y.; Yarita, T. *J. Chromatogr., A* **2006**, *1131*, 285−288.
(15) Cai, S.-S.; Syage, J. A.; Hanold, K. A.; Balogh, M. P. *Anal. Chem.* **2009**, *81*, 2123−2128.
(16) Bagag, A.; Giuliani, A.; Lapŕevote, O. *Int. J. Mass Spectrom.* **2007**, *264*, 1−9.
(17) Ǵomez-Ariza, J. L.; Garćıa-Barrera, T.; Lorenzo, F. *Anal. Chim. Acta* **2006**, *570*, 101−108.
(18) Mohameda, R.; Hammela, Y.-A.; LeBreton, M.-H.; Tabet, J.-C.; Jullien, L.; Guy, P. A. *J. Chromatogr., A* **2007**, *1160*, 194−205.
(19) Takino, M.; Daishima, S.; Nakahara, T. *Rapid Commun. Mass Spectrom.* **2003**, *17*, 1965−1972.
(20) Takino, M.; Yamaguchi, K.; Nakahara, T. *J. Agric. Food Chem.* **2004**, *52*, 727−735.
(21) Takinoa, M.; Daishimab, S.; Nakaharac, T. *J. Chromatogr., A* **2003**, *1011*, 67−75.
(22) Lembcke, J.; Ceglarek, U.; Fiedler, G. M.; Baumann, S.; Leichtle, A.; Thiery, J. *J. Lipid Res.* **2005**, *46*, 21−26.
(23) Cai, S.-S.; Short, L. C.; Syage, J. A.; Potvin, M.; Curtis, J. M. *J. Chromatogr., A* **2007**, *1173*, 88−97.
(24) Lagalante, A. F.; Oswald, T. D. *Anal. Bioanal. Chem.* **2008**, *391*, 2249−2256.
(25) Robb, D. B.; Blades, M. W. *Anal. Chim. Acta* **2008**, *627*, 34−49.
(26) Kauppila, T. J.; Kuuranne, T.; Meurer, E. C.; Eberlin, M. N.; Kotiaho, T.; Kostiainen, R. *Anal. Chem.* **2002**, *74*, 5470−5479.
(27) Raffaelli, A.; Saba, A. *Mass Spectrom. Rev.* **2003**, *22*, 318−331.
(28) Kauppila, T. J.; Kostiainen, R.; Bruins, A. P. *Rapid Commun. Mass Spectrom.* **2004**, *18*, 808−815.

(29) Kauppila, T. J.; Kotiaho, T.; Kostiainen, R.; Bruins, A. P. *J. Am. Soc. Mass Spectrom.* **2004**, *15*, 203−211.
(30) Syage, J. A. *J. Am. Soc. Mass Spectrom.* **2004**, *15*, 1521−1533.
(31) Kauppila, T. J.; Bruins, A. P.; Kostiainen, R. *J. Am. Soc. Mass Spectrom.* **2005**, *16*, 1399−1407.
(32) Purcell, J. M.; Hendrickson, C. L.; Rodgers, R. P.; Marshall, A. G. *J. Am. Soc. Mass Spectrom.* **2007**, *18*, 1682−1689.
(33) Short, L. C.; Cai, S.-S.; Syage, J. A. *J. Am. Soc. Mass Spectrom.* **2007**, *18*, 589−599.
(34) Short, L. C.; Hanold, K. A.; Cai, S.-S.; Syage, J. A. *Rapid Commun. Mass Spectrom.* **2007**, *21*, 1561−1566.
(35) Kamel, A.; Jeanville, P.; Colizza, K.; J-Rivera, L. E. *J. Am. Soc. Mass Spectrom.* **2008**, *19*, 1579−1589.
(36) Panda, S. K.; Brockmann, K.-J.; Benter, T.; Schrader, W. *Rapid Commun. Mass Spectrom.* **2011**, *25*, 2317−2326.
(37) Hehre, W. J.; Ditchfield, R.; Pople, J. A. *J. Chem. Phys.* **1972**, *56*, 2257−2261.
(38) Gonzalez, C.; Schlegel, H. B. *J. Chem. Phys.* **1991**, *95*, 5853−5860.
(39) Schmidt, M. W.; Baldridge, K. K.; Boatz, J. A.; Elbert, S. T.; Gordon, M. S.; Jensen, J. H.; Koseki, S.; Matsunaga, N.; Nguyen, K. A.; Su, S.; Windus, T. L.; Dupuis, M.; Montgomery, J. A. *J. Comput. Chem.* **1993**, *14*, 1347−1363.
(40) Wiberg, K. B. *Chem. Rev.* **1955**, *55* (4), 713−743.
(41) *NIST Chemistry Webbook*, NIST Standard Reference Database Number 69; Mallard, W. G., Linstrom, P. J., Eds.; National Institute of Standards and Technology: Gaithersburg, MD, 20899, July 2001; http://webbook.nist.gov.